Enhanced depressurisation for methane recovery from gas hydrate reservoirs by injection of compressed air and nitrogen

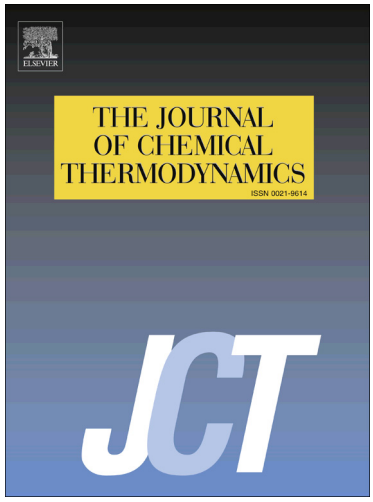

Enhanced Depressurisation for Methane Recovery from Gas Hydrate Reservoirs by Injection of Compressed Air and Nitrogen

Anthony Okwananke, Jinhai Yang, Bahman Tohidi, Evgeny Chuvilin, Vladimir Istomin, Boris Bukhanov, Alexey Cheremisin

PII: S0021-9614(17)30353-1
DOI: https://doi.org/10.1016/j.jct.2017.09.028
Reference: YJCHT 5227

To appear in: *J. Chem. Thermodynamics*

Received Date: 31 May 2017
Revised Date: 22 September 2017
Accepted Date: 23 September 2017

Please cite this article as: A. Okwananke, J. Yang, B. Tohidi, E. Chuvilin, V. Istomin, B. Bukhanov, A. Cheremisin, Enhanced Depressurisation for Methane Recovery from Gas Hydrate Reservoirs by Injection of Compressed Air and Nitrogen, *J. Chem. Thermodynamics* (2017), doi: https://doi.org/10.1016/j.jct.2017.09.028

Enhanced Depressurisation for Methane Recovery from Gas Hydrate Reservoirs by Injection of Compressed Air and Nitrogen

Anthony Okwananke[a], Jinhai Yang[a*], Bahman Tohidi[a], Evgeny Chuvilin[b], Vladimir Istomin[b], Boris Bukhanov[b], Alexey Cheremisin[b]

[a] Centre for Gas Hydrate Research, Institute of Petroleum Engineering, Heriot-Watt University, Edinburgh, EH14 4AS, United Kingdom
[b] Centre for Hydrocarbon Recovery, Skolkovo Institute of Science and Technology, Moscow, Russia

ABSTRACT

Enhanced depressurisation for methane recovery from gas hydrate-bearing sediments was experimentally studied by injection of compressed air and nitrogen. Experiments were conducted in simulated sediments (silica sand) from 273.4 K to 283.0 K and initial system pressures ranging from 3.8 MPa to 7.2 MPa before air or nitrogen injection. The results show that injection of air and nitrogen made it possible to implement conventional depressurisation in multiple stages. In each pressure stage, methane hydrate was quickly dissociated by the injected air or nitrogen due to direct shift of the methane hydrate equilibrium phase boundary. Methane hydrate dissociation at high pressures enables methane recovery inside the methane hydrate stability zone. Depressurisation well above the methane hydrate dissociation pressure generated a methane-rich gas phase of up to 90 mol% methane depending on the injected gas. Injection of compressed air or nitrogen provides a potential approach to improve the technical feasibility and economic viability of conventional depressurisation method for methane recovery from most gas hydrate reservoirs with severe conditions such as low permeability or dispersed hydrates.

Keywords: *Gas hydrate; methane recovery; compressed air; nitrogen; kinetics; depressurisation*.

* Corresponding author: petjy@hw.ac.uk

1. Introduction

Natural gas, the cleanest burning of all fossil fuels holds the key to reduced CO_2 emissions in the immediate and near future. The use of natural gas in place of high carbon energy sources therefore requires abundance of natural gas sources. Natural gas hydrate (NGH) reserves could play a significant role in this regard. Natural gas hydrates belong to a group of compounds known as clathrate hydrates. Clathrate hydrates are solid inclusion compounds in which water molecules forms a crystalline lattice composed of cavities occupied by suitably sized guest molecules, mostly gas and volatile liquids [1]. It is abundant in nature, with reserves of over 1.5×10^{15} m^3 of hydrate-bounded methane [2-4]. It has been touted as a potential future energy source. This has elicited interest in the development of techniques to economically exploit the resource given its unconventional nature and its harsh habitat. It occurs mainly in permafrost and in continental shelves of the world's oceans. It is composed chiefly of methane and other components of natural gas including ethane, propane, carbon dioxide, and hydrogen sulphide depending on the source gas for hydrate formation [5]. They are stable under conditions of high pressure and low temperature, thus decompose into the constituent water and gas when any perturbation results in shifting the local equilibrium away from the hydrate stability zone (HSZ). This has been the basis of the widely-reported techniques for gas recovery from NGH reservoirs such as depressurisation, thermal stimulation, and chemical inhibitor injection. Gas injection leverages on the difference in chemical potential between the injected gas and the hydrate phase to decomposed NGH.

Depressurisation reduces the reservoir pressure beyond the hydrate stability zone to initiate hydrate dissociation [6-9]. The depressurisation technique is the most promising in terms of practicality and economics. It has been applied successfully to produce gas in commercial quantities from the Messoyakha gas field in the Russian Arctic [10]. A number of field trials for scientific and engineering studies also employed the depressurisation technique. The

Mallik 2007/2008 successfully demonstrated that depressurisation only can be used to produce gas from gas hydrate reservoir [11]. In the same vein, depressurisation was also employed in the first offshore production test in eastern Nankai Trough, Japan [12]. The reported field production tests were conducted in arctic sandstones and deep-water sandstones with good reservoir quality and significant hydrate saturations. In reality, only a small proportion of known hydrate reserves are found in sediments with good reservoir quality. Majority of hydrate reserves is found in fine-grained low permeability sediments with very low and dispersed hydrate saturation [13]. Thus, for these types of reservoirs, economic recovery of gas by depressurisation is not feasible. Also, for hydrate reservoir far inside the HSZ, a high extent of depressurisation is needed to dissociate hydrate. Traditionally, depressurisation encounters excessive water production and sand migration which blocks production facilities. This reportedly led to the termination of the offshore production trail in the eastern Nankai Trough, Japan [12] and the Mallik 2007 production test [11].

Thermal stimulation increases the reservoir temperature beyond the HSZ thereby leading to hydrate dissociation [14-17]. Heat energy is supplied in the form of steam injection or hot water injection [18, 19]. Major disadvantages of this technique are reduced efficiency due to the loss of heat energy during delivery from source to the reservoir [15]. The injection of inhibitors such as methanol and monoethylene glycol (MEG) alters the hydrate phase boundary chemically to dissociate the hydrate [20-22]. However, huge volumes of chemicals would be needed to dissociate hydrate for substantial gas recovery. Also, such injected chemical is potentially harmful to the environment.

The concept of methane recovery from CO_2 injection into methane hydrate has been studied extensively [16-19]. CO_2-CH_4 exchange is favoured thermodynamically as the exothermic heat of CO_2-hydrate formation is greater than the endothermic heat of methane hydrate

dissociation. Though it is not yet understood which of these two processes takes precedence over the other. The process has the benefit of sequestering CO_2 as CO_2-hydrate while recovering methane. Also, the CO_2-hydrate formed helps in reducing water production and maintaining the integrity of the formation after methane hydrate dissociation. However, CO_2 injection could lead to secondary CO_2-hydrate formation, hindering further CO_2-CH_4 replacement if the CO_2 hydrate coats the methane hydrate crystals and also reducing formation permeability if the CO_2 hydrate clogs pores. CO_2-hydrate could form at the base of the hydrate stability zone, acting as a seal for upward migrating CO_2 in a geological CO_2 sequestration process [23]. Thus, if such a system is coupled with natural gas recovery from natural gas hydrate reservoir, the CO_2-hydrate formed could also act as a barrier to the recovery of natural gas released. Moreover, given the harsh conditions in which gas hydrates occurs naturally, injected CO_2 gas will be converted into liquid CO_2, reducing the soaking, speed of migration thereby negatively affecting the injectivity and diffusion of CO_2 [24].

The introduction of a second gas (nitrogen) in mixture with CO_2 has been shown to increase the recovery of methane in methane hydrate by enhancing CO_2 replacement. Park et al. [24] and Kang et al. [25] showed that a mixture of 20% CO_2 and 80% nitrogen gave a methane recovery of 85% as compared to 64% obtained when only CO_2 was used. In crystallographic studies of CH_4-(N_2+CO_2) exchange in sH methane hydrate, Shin et al. [26] reported that nitrogen significantly influenced a structural transition from sH to sI and consequently enabled more than 92% methane recovery. Recently, Lee et al. [27] in a similar study reported a 74% flue gas replacement of CH_4-neohexane structure H (sH) hydrates, however, without any structural transition. A CO_2 replacement field trial was conducted at Ignik Sikumi, North Slope, Alaska [28]. The injected CO_2 stream contained 77% N_2 to prevent secondary CO_2-hydrate formation especially near the wellbore and to achieve optimum CO_2-CH_4 replacement. Approximately 6000 m^3 of (N_2+CO_2) gas was injected while about 30000

m^3 of gas was produced over a five-week period. About half of the 1400 m^3 of injected CO_2 was sequestered. However, about 50% of the produced gas could not be recovered until the reservoir was depressurized below the HSZ [29]. Haneda et al. [30] and Panter et al. [31] showed that nitrogen and oxygen can dissociate methane hydrate due to chemical potential difference between their gas and solid hydrate phases. Kang et al. [32] and Ahn [33] conducted an air-CH_4 exchange experiment. They reported the existence of a critical methane concentration that serves as the boundary between decomposition and replacement in methane hydrate reservoir. They also observed that the addition of CO_2 to the injected air resulted in the occurrence of a strong and stable self-regulating exchange process.

The inherent deficiencies in these techniques making them inefficient for economic gas production has been highlighted. However, it is a general consensus that depressurisation is the most technically feasible for economic recovery, thus it is the most combined with other methods. The huff and puff technique demonstrated by Li et al. [34] is a combination of thermal stimulation and depressurisation involving cycles of injection of hot fluid (water or steam), soaking, and gas production. According to the authors gas to water ratio of 55 m^3 of methane (STP)/m^3 of water justifies the economic feasibility of the process. Steam Assisted Gravity Drainage (SAGD) [35] and Steam Assisted Antigravity Drainage (SAAD) [36] have also been tested for gas recovery from natural gas hydrates in sediments in a combination of thermal stimulation, depressurisation, and brine injection. Both methods employ two horizontal wells; one injection and one production. In our recent studies [37, 38], we demonstrated that the extent of depressurisation could be reduced thus, avoiding depressurizing below the methane HSZ. It was shown that depressurising in the presence of flue gas could generate as high as 80 mol% methane in the gas phase at pressures above the methane hydrate dissociation pressure. This could potentially help in avoiding the problems associated with depressurisation below the HSZ.

In our previous study [37, 38], we showed that flue gas injection could recover methane from gas hydrate reservoirs with the added benefit of CO_2 sequestration. However, sources of flue gas are seldom close to the point of injection into gas hydrate reservoirs, therefore requiring additional cost for transportation through pipelines. In contrast, air is readily available and could be compressed on-site for direct injection. In this study, we investigated a new approach to enhance the depressurisation process for methane recovery by injection of compressed air. It is noted that injecting a gas mixture containing oxygen into gas hydrate reservoirs poses some potential problems. Oxygen catalyses corrosion and rust well casings and other metallic conduits. Moreover, oxygen containing gas mixtures is potentially flammable. Installation of a membrane separator could help in producing an oxygen-depleted air for injection. Puri and Yee [39] developed a method to recover methane from coalbed methane by injecting an oxygen-depleted air (i.e., the effluent of an air stream passed through a membrane separator) into the coalbed formation. In this vein, we also investigated nitrogen injection at similar condition for comparison with air injection.

2. Method

The main components of air are nitrogen and oxygen, typically about 79% nitrogen and 21% oxygen. Both are similar in hydrate forming characteristics. They are small sized molecules of molecular diameter 4.1 Å and 4.2 Å respectively, forming structure II (sII) hydrate, requiring a higher hydrate formation pressure compared to methane hydrate and CO_2 hydrate (structure I) at the same temperature as shown by the equilibrium phase boundaries of nitrogen-, oxygen-, methane-, and CO_2-hydrates in Figure 1a predicted by an in-house thermodynamic model HydraFLASH [40].

Panter et al. [31] showed that increasing the amount of nitrogen in the gas phase of nitrogen + methane hydrate system, and nitrogen + methane + ethane hydrate system shifts the equilibrium phase boundary to conditions of higher pressures and lower temperatures. Thus,

nitrogen creates low partial pressure hence a chemical potential imbalance between methane in the hydrate and in the gas phase and could therefore dissociate methane hydrate. In this vein therefore, methane hydrate reservoir conditions shift outside the methane HSZ leading to the dissociation of methane hydrate, depending on the pressure of air/nitrogen injected into a methane hydrate reservoir. Methane hydrate decomposes into water and methane. Figure 1b shows the predicted HSZs of air hydrate, methane hydrate in the presence of different amounts of air in equilibrium with the system. It is seen that 80 mol% of air can shift the methane hydrate phase boundary from 2.7 MPa to 8.3 MPa at 273 K and from 4.3 MPa to as high as 13.7 MPa at 278 K. The ratio of methane in the gas phase increases gradually as more methane is released due to hydrate decomposition. Methane decomposition continues, controlled by heat and mass transfer until the amount of methane in the vapour phase is sufficient to achieve a new thermodynamic equilibrium in the presence of air/nitrogen. It is expected that mixed hydrates such as N_2-CH_4, O_2-CH_4, and N_2-O_2-CH_4 form. However, at typical gas hydrate reservoir conditions e.g., 273.3 K to 284.2 K and 4.2 MPa to 13.8 MPa [33, 34], and the limitation of air injection pressure would not provide sufficient driving force for the formation of N_2-CH_4 and N_2-O_2-CH_4 mixed hydrate. Therefore, the presence of air (N_2 and O_2) only destabilises the balance of chemical potential of methane between the hydrate and the gas phases thereby decomposing the hydrate. Similar behaviour is exhibited by nitrogen.

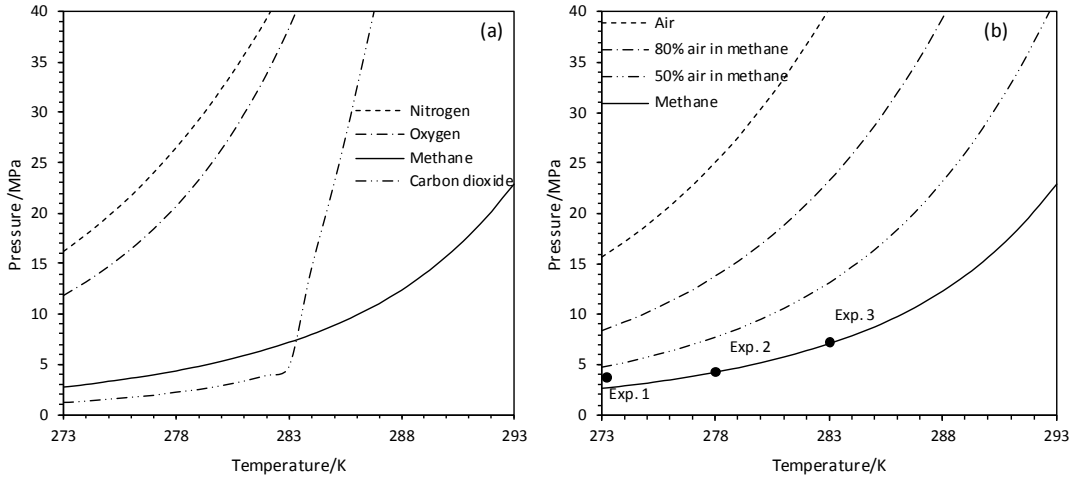

Figure 1 (a) Equilibrium phase boundaries of nitrogen-, oxygen-, methane-, CO_2-hydrates; (b) Predicted shifts in methane hydrate stability zone due to compressed air injection and the experiment conditions. The phase boundaries were predicted by HydraFLASH [40].

3. Experimental Section

3.1 Materials

Silica sand (Fife, Scotland) with particle size ranging from 1.2 µm to 600 µm and an average diameter of 256.5 µm was used to simulate the porous medium. Distilled water was used to partially saturate the silica sand. Methane, nitrogen and oxygen used were supplied by BOC Ltd (Table 1). Nitrogen and oxygen gas were used to synthesize the compressed air composed of 80 mol% N_2 and 20 mol% O_2, which was analyzed by a gas chromatograph.

Table 1 Purity of gases used

Chemical	Source	Mole fraction purity
Methane	BOC	0.99995
Nitrogen	BOC	0.99998
Oxygen	BOC	0.996

3.2 Experimental apparatus

Figure 2 is a schematic view of the experimental rig. It consists of a high-pressure piston cell made of 316 stainless steel. The cell maximum height is 18.2 cm and an inner diameter of 7.5 cm with a maximum working volume of 800 cm^3. The maximum working pressure is up to 40 MPa and is housed in a rectangular jacket made of aluminum. The jacket has two openings, an inlet, and an outlet through which a cooling fluid circulates. The cooling fluid is supplied by a cryostat, Grant LTC with working temperature ranging from 253 to 323 K. The temperature of the cell was measured with a Platinum Resistant Thermometer (PRT) coated in stainless steel and has an uncertainty of 0.1 K. Cell pressure was measured using a Quartzdyne series I pressure transducer with an uncertainty of 0.05 MPa. At the bottom end of the cell a movable piston can simulate overburden, vary cell pressure and/or volume as desired by moving forward or backward with the injection or withdrawal of hydraulic fluid, which is driven by a hydraulic pump. A displacement meter (Linear Variable Differential Transformer – LVDT) fitted to the tail rod of the piston enables the measurement of piston displacement. This aids in estimation determination of the volume of the cell at any position. The overburden pressure was measured by a Druck pressure transducer with an accuracy of 0.05 MPa connected to the back of the piston. The cell pressure, temperature, overburden pressure, and piston displacement are monitored by LabView software interface (National Instruments) and recorded on a computer at 60 seconds interval via a Data Acquisition System (DAS) from National Instruments.

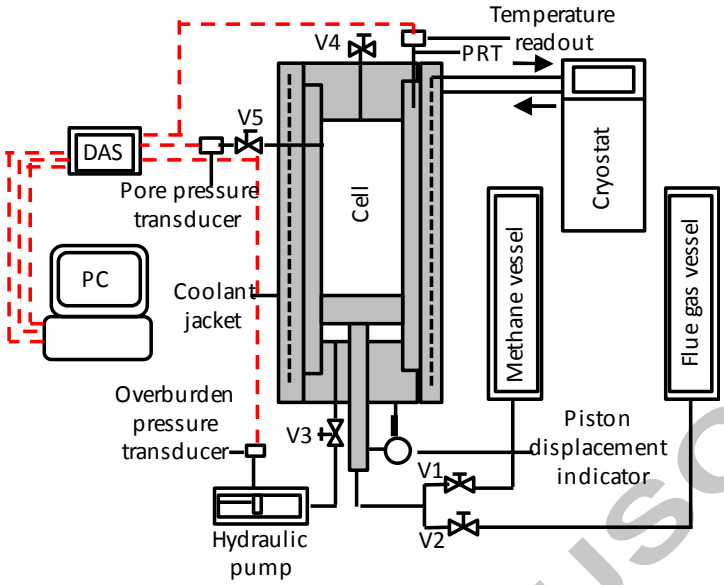

Figure 2 Schematic diagram of the experimental rig

3.3 Methane hydrate formation

The silica sand was dried in an oven (Stuart Scientific) at 373 K for 24 hours. After the dried sand was cooled to room temperature at about 293 K, a predetermined quantity of deionised water was then added in the sand to a desired water saturation. The sand and water was manually mixed thoroughly to ensure the added water evenly distributes in the partially saturated sand. The partially water-saturated sand was charged into the cell and vacuumed. An overburden pressure of 3.5 MPa was applied by pushing the piston upward to compress the mixture. Methane gas was then injected into the cell through valve V1 as shown in Figure 2 to pressurise the system at ambient temperature (293 K). The temperature of the cell was then maintained at 293K and allowed the system to equilibrate. Once equilibrium was achieved, cell temperature was set to 273.4 K to initiate methane hydrate formation. Figure 3 shows a typical pressure profile with temperature during hydrate formation. Pressure decreased starting from point A as temperature decreased due to change in gas solubility in water and gas contraction upon cooling. At point B, a change in slope is observed due to sudden drop in pressure. This pressure drop indicates hydrate nucleation. The pressure drop

continues as the hydrate nuclei continue to grow to reach a critical size. At point C, the hydrate nuclei have achieved stability and a rapid pressure drop is observed as the stable hydrate nuclei grows into solid hydrate. The rapid pressure drop continues until the maximum sorption is achieved at point D. At point D, pressure change ceased, indicating the completion of hydrate formation. The amount in mole of methane consumed for methane hydrate formation can be simply computed from the generic equation below:

$$n_{\mathrm{i(con)}} = \left(\frac{PV}{zRT}\right) y_{\mathrm{i,t=0}} - \left(\frac{PV}{zRT}\right) y_{\mathrm{i,t=t}} \tag{1}$$

where $n_{i(con)}$ is the number of moles of component i consumed, P is the system pressure, V is the volume of the vapour phase, z is the compressibility factor, R is the gas constant, T is the system temperature, y_{i} is the mole fraction of component $'\mathrm{i}'$ in the gas phase, and t is time. Component $'\mathrm{i}'$ in this case is methane. The compressibility factor z was computed using Peng-Robinson (PR) equation-of-state [41]

It was however noted that non-zero water saturations were achieved at the end of hydrate formation in all experiments despite the presence of free gas. This may be attributed to the fact that the remaining water could be wrapped by methane hydrate crusts. The hydrate crusts separate the remaining water from the remaining methane gas, therefore, hindering mass transfer between the water and the gas hence further hydrate formation.

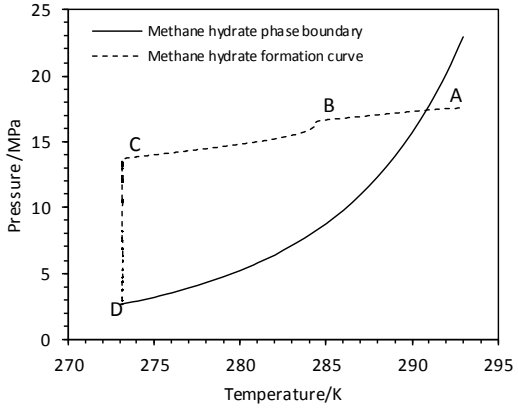

Figure 3 Methane hydrate phase boundary and pressure profile during methane hydrate formation.

3.4 Methane recovery

After the completion of hydrate formation, compressed air was injected in excess to purge the remaining methane gas. The cell was purged of the excess gas mixture until the cell pressure was about 0.7 MPa higher than the air- and nitrogen- hydrate dissociation pressure. This was to minimize any possible methane hydrate dissociation. Methane recovery was conducted in multi-pressure stages. In each stage, the system was set to a target pressure corresponding to the desired vapour phase composition at equilibrium by returning the piston, which expanded the cell volume, reducing the system pressure without any need for fluid withdrawal from the test cell. The time at which the desired target pressure was reached in each stage was taken as time zero, that is, the commencement of methane recovery for that stage. Samples from the vapour phase were taken and analysed for composition using a gas chromatograph (Varian 3600). Cell pressure drops during sampling by a maximum of about 0.015 MPa which did not lead to any significant change in the system. Sampling and compositional analysis in each stage continued until there was no noticeable change in the vapour phase composition of methane. At this point, the system was considered to have reached equilibrium. The amount in mole of methane released from methane hydrate, cumulated over the stages was also computed using Equation 1 in reverse. The rate of methane release from the hydrate phase in each of the stages was calculated by:

$$\frac{dn_{\mathrm{i}}}{dt} = \frac{(n_{\mathrm{i,G}})_{\mathrm{t}+\Delta\mathrm{t}} - (n_{\mathrm{i,G}})_{\mathrm{t}=0}}{\Delta t} \tag{2}$$

where $(n_{i,G})_{t+\Delta t}$ is the mole of methane in the vapour phase at the end of the stage, $(n_{i,G})_{t=0}$ is the mole of methane in the vapour phase at the commencement of the stage, and Δt is the time duration of the stage.

4 Results and Discussions

The experiments are composed of two parts. The first part was designed to study the kinetics of methane recovery in the presence of air and nitrogen during the multi-stage depressurisation. It was designed to achieve 50-60 mol% methane in the gas phase. In the second part, the multi-stage depressurisation continued to achieve maximum methane recovery. Two fundamental issues were investigated: methane hydrates decomposition behaviour in the presence of air or nitrogen, and how injection of air or nitrogen enhances the depressurisation process. Table 2 is a summary of the initial conditions of the hydrate-bearing sediment before gas injection. The table presents the test temperatures, equilibrium pressures after hydrate formation, hydrate saturation S_h, gas saturation S_g, and water saturation S_w. A hydration number of 6.0 was used in calculation of methane hydrate saturation [1].

Table 2 Summary of the initial conditions of the hydrate-bearing sediments before compressed air injection, nitrogen, and flue gas injection.[a]

Exp.	*T*/K	*P*/MPa	ϕ/%	S_h/vol%	S_g/vol%	S_w/vol%
1 (air)	273.4	3.8	37.4	67.8	22.5	9.6
2 (air)	278.0	4.3	37.4	74.6	21.4	4.1
3 (air)	283.0	7.2	37.3	61.0	23.7	15.3
4 (N_2)	273.4	5.5	37.3	62.3	22.1	15.6

[a] $U(T)$ = 0.1 K, $U(P)$ = 0.05 MPa, $U_r(\phi)$ = 1%, $U_r(S_h)$ = $U_r(S_g)$ = $U_r(S_w)$ = 3.5%. (0.95 level of confidence).

4.1 Multi-stage depressurisation

Changing vapour phase composition with time was used to monitor the release of methane from the hydrate phase into the vapour phase after injection of air or nitrogen. Methane hydrate decomposition commenced immediately once the system pressure dropped below the

air-, and nitrogen-hydrate phase boundary at the experimental temperature. This immediate decomposition enabled the implementation of multi-stage depressurisation in the presence of air/nitrogen. The typical kinetic process of methane hydrate decomposition after air/nitrogen injection is shown in Figure 4 for Experiment 2. At the beginning of each stage, fast methane hydrate decomposition was observed, which is shown by the nearly vertical portion of the curves. This was followed by a slow decomposition which eventually ceases with time as the system achieves a new thermodynamic equilibrium. Similar trends were also observed in the other experiments.

Graphical representation of the vapour phase concentrations is shown in Figure 5. The figures show that the air and nitrogen components of the vapour phase varies inversely with that of methane. The ratio $N_2/(N_2+O_2)$ was used to indicate the composition of the individual components of air in the vapour phase in Experiment 1, 2, and 3, respectively. It is seen in Figure 7 (a), (b), and (c) that $N_2/(N_2+O_2)$ remains constant throughout the duration of the experiments. This indicates that there is no preferential inclusion of one of the components of air into the hydrate phase over the other.

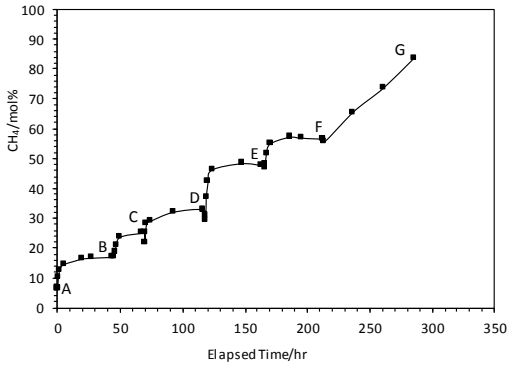

Figure 4 Methane recovery stages after air/nitrogen injection showing the multi-stage depressurisation (Experiment 2). A-B, B-C, C-D, D-E, E-F, F-G represents Stages 1, 2, 3, 4, 5, and 6 respectively. Kinetic measurements were made in Stages 1-5.

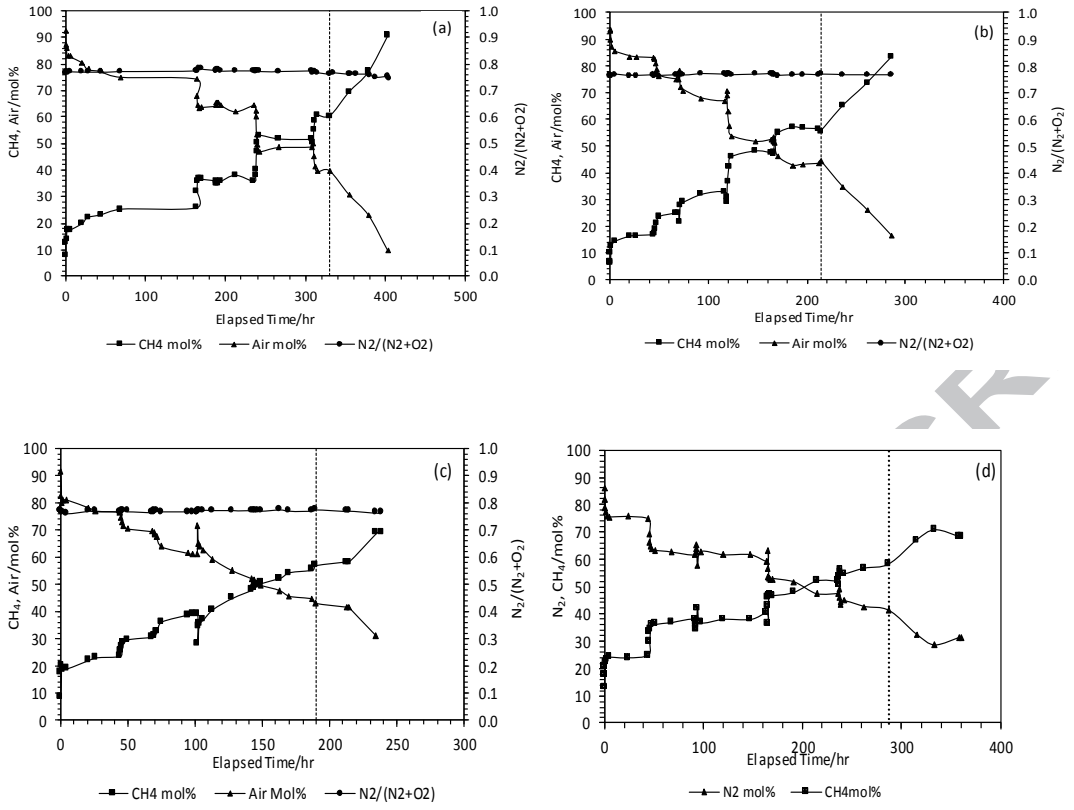

Figure 5 Gas phase composition showing methane concentration in the experiments with air (a), (b), (c), and nitrogen (d). $N_2/(N_2+O_2)$ in (a), (b), (c) shows that the relative ratio of N_2 and O_2 in the gas phase remains approximately constant.

4.2 Kinetics of methane recovery

Methane hydrate decomposition was achieved by the equilibrium phase boundary shift in the presence of the injected gas from a methane-lean region to a methane-rich region. Table 3 shows the initial pressure, set pressure for dissociation, pressure reached at equilibrium and gas phase methane concentration achieved in each of the pressure stage for the experiments. In Table 3, at the end of Stage 5 in each experiment, the system was set to a pressure for the target gas phase methane concentration and allowed enough time to reach equilibrium afterwards, gas phase methane concentrations of 60.3 mol%, 56.5 mol%, 55.3 mol%, and 58.5 mol%, respectively.

Table 3 Initial pressure, set pressure, equilibrium pressure, and vapour phase methane concentration.[a]

Exp.	T /K	Stage	Initial P /MPa	Set P /MPa	P at equilibrium /MPa	Methane /mol%
1 (air)	273.4	0	15.0	-	-	12.7
		1	15.0	11.4	8.0	25.7
		2	8.0	6.3	6.6	35.8
		3	6.6	5.7	5.9	38.6
		4	6.0	4.2	4.8	51.4
		5	4.8	3.9	4.2	60.3
2 (air)	278.0	0	23.6	-	-	6.6
		1	23.6	17.3	16.7	16.9
		2	16.7	12.3	12.9	24.9
		3	12.9	10.5	11.0	32.9
		4	11.1	7.4	8.4	47.6
		5	8.4	6.7	7.3	56.5
3 (air)	283.0	0	38.5	-	-	8.6
		1	38.5	27.0	26.9	23.5
		2	26.9	18.8	19.9	30.6
		3	19.9	15.9	16.6	39.2
		4	16.8	11.8	13.4	47.9
		5	13.4	10.5	11.2	55.3
4 (N_2)	273.4	0	17.2	-	-	13.6
		1	17.2	11.9	11.7	25.1
		2	11.7	9.0	9.3	38.2
		3	9.3	7.8	8.1	40.5
		4	8.4	5.7	6.2	52.1
		5	6.2	4.9	5.2	58.5

[a] $U(T)$ = 0.1 K, $U(P)$ = 0.05 MPa, U_r(methane concentration) = 2%. (0.95 level of confidence).

The amount of methane released in each stage in Experiments 1-4 (air, nitrogen injection) is shown in Figure 6. It was cumulated from Stage 1 to Stage 5 in each experiment. Furthermore, methane release could also be divided into two sub-stages: a first sub-stage in which methane release was rapid and a second sub-stage in which methane release rate became a few orders of magnitude lower until a new equilibrium was reached. For example, in Stage 1 of the multi-stage depressurisation phase at 278 K (Experiment 2), of a total of 0.15 mole of methane released as shown in Figure 7, 0.12 mole was released during the first 5

hours, representing 80% of total mole released. The remaining 0.03 mole representing only 20% of total mole released was released for the rest of the time as the system reached a new thermodynamic equilibrium.

Table 4 is a summary of recovery experiments during the multi-pressure depressurisation phase showing rate of methane release, amount of methane released from methane hydrate and percentage methane recovery. Equation 2 was used to calculate the rate of methane release. The amount of methane released from the hydrate phase into the gas phase during the first phase of the multi-stage depressurisation increased from 0.10 mole to 0.41 mole in Experiment 1, 0.15 mole to 0.75 mole at Experiment 2, 0.29 mole to 0.84 mole in Experiment 3 and 0.12 mole to 0.64 mole in Experiment 4. These correspond to recoveries of 38.0%, 64.4%, 96.9% and 67.9%, respectively. This is in spite of the gas phase methane concentration at the end of this recovery phase being slightly higher in Experiment 1 (60.3 mol%) than in Experiment 2 (56.5 mol%), Experiment 3 (55.3 mol%) and Experiment (58.5 mol%). The increasing amount of methane recovery with temperature is attributed to hydrate equilibrium pressure. At higher temperatures, the hydrate equilibrium pressure is higher, implying a higher gas phase density in equilibrium with the hydrate phase. Therefore, to achieve a given vapour phase methane concentration, more methane needs to be released from the hydrate at higher temperature than at lower temperatures.

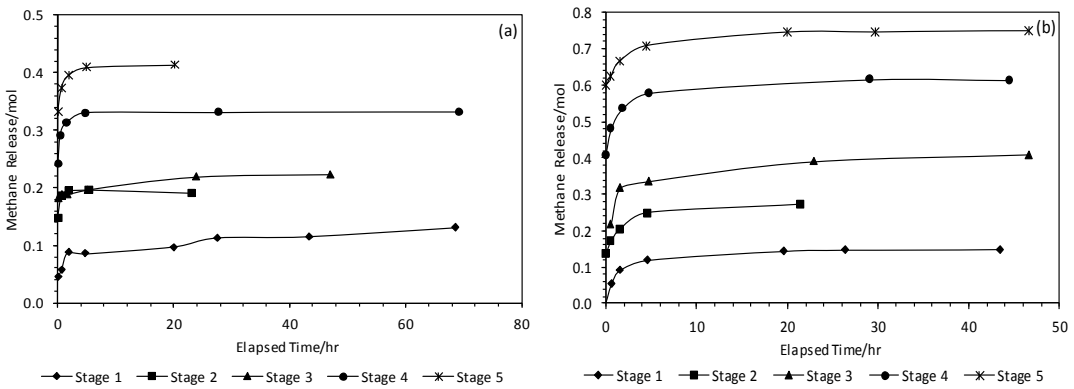

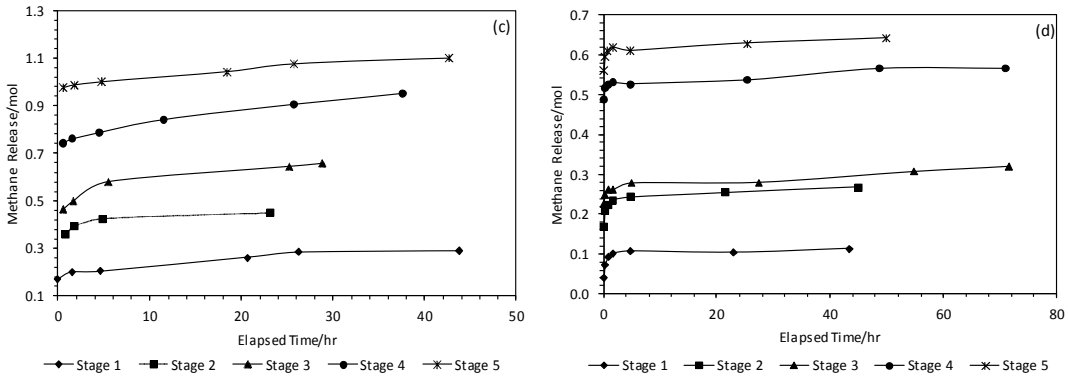

Figure 6 Amount of methane released from the hydrate phase into the gas phase in each stage of the multi-stage depressurisation. (a), (b), (c) represent Experiments 1, 2, and 3 (air injection) conducted at 273.4 K, 278 K and 283 K respectively. (d) represents Experiment 4 (nitrogen injection) conducted at 273.4 K.

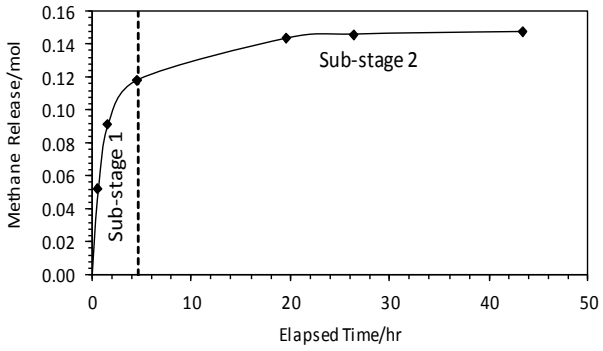

Figure 7 Methane release in Stage 1 of the multi-stage depressurisation at 278 K (Experiment 2). 0.12 mole out of 0.15 mole total corresponding to 80% was released from 0-5 hours.

Table 4 Summary of recovery experiments during the multi-stage depressurisation phase showing rate of methane recovery, amount of methane released from methane hydrate and percentage methane recovery.[a]

Exp.	*T* /K	Stage	Recovery rate/mol/hr		Amount released /mole	Methane recovery /%
			Sub-stage 1	Sub-stage 2		
		1	0.0246	0.0007	0.10	9.2

		2	0.0227	0.0003	0.19	17.5
1 (air)	273.4	3	0.0034	0.0008	0.22	20.5
		4	0.0455	0.0005	0.33	30.4
		5	0.0343	0.0008	0.41	38.0
		1	0.0555	0.0013	0.15	12.6
		2	0.0416	0.0027	0.27	23.3
2 (air)	278.0	3	0.0904	0.0017	0.41	35.0
		4	0.0646	0.0015	0.61	52.8
		5	0.0441	0.0023	0.75	64.4
		1	0.116	0.0034	0.29	33.1
		2	0.0418	0.0013	0.45	51.4
3 (air)	283.0	3	0.0301	0.0033	0.66	75.4
		4	0.0613	0.0052	0.84	96.9
		1	0.0309	0.00019	0.12	12.2
		2	0.0323	0.00069	0.27	28.5
4 (N_2)	273.4	3	0.017	0.00075	0.32	34.0
		4	0.0195	0.00061	0.57	60.0
		5	0.0269	0.00056	0.64	67.9

[a] $U(T)$ = 0.1 K, U_r(recovery rate) = U_r(amount released) = 7.5%, U_r(methane recovery) = 8.5%. (0.95 level of confidence)

Noting that the experiments were set in an isochoric system, methane release from methane hydrate was therefore monitored by the increasing system pressure as well as the increasing gas phase methane concentration. Contrary to expectation, at the end Stage 1 in Experiments 1 to 4, the system pressure at equilibrium was less than the set pressure at the commencement of the recovery experiment. On setting the system pressure to the desired set point, it was observed that as the system pressure dropped below the air/nitrogen phase boundary, there was an initial surge in pressure due to rapid methane hydrate decomposition which lasted only a short time. This was followed by a gradual and continuous decrease in pressure despite increasing gas phase methane concentration. At this time, the system is dominated by the inclusion of air/nitrogen into the hydrate phase as the set pressure at Stage 1 is close to the air/nitrogen hydrate phase boundary. Thus, the continued increase in the gas phase methane concentration is as a result of the reduction in the amount of the air/nitrogen component of

the gas phase rather than methane hydrate decomposition. In Stages 2-5 in the Experiments, as expected, the equilibrium pressure at the end of each stage increased from the set pressure at the commencement of recovery in each stage. In Stages 2-5, the set pressure was far and below the air/nitrogen hydrate equilibrium phase boundary, thus, methane hydrate dissociation dominated as evident in the simultaneous increase in system pressure and gas phase methane concentration. The pressure profiles for Experiment 2 is shown in Figure 8. Similar trends were observed for Experiments 1, 3, and 4.

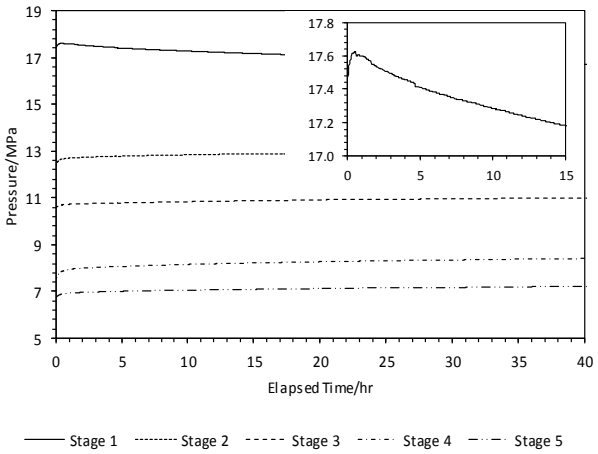

Figure 8 Pressure profiles of Stages 1-5 of the multi-stage depressurisation (Experiment 2 at 278 K). The inset highlights the initial surge in pressure followed by the gradual decrease in pressure in Stage 1.

4.3 Enhanced depressurisation for methane recovery

For maximum methane recovery after the first phase of the multi-stage depressurisation, the system was subjected to further depressurisation in stages. Each stage lasted 24 hours to ensure equilibrium was reached. Figure 9 is a plot of the gas phase methane concentrations versus pressure during the entire depressurisation phases. The dashed vertical lines represent the dissociation pressure lines of methane hydrate at the corresponding experimental temperatures. In Experiments 2 and 3, the maximum gas phase methane concentrations, 84

mol% and 69 mol% respectively were achieved before the methane hydrate dissociation pressure was reached at 4.87 MPa in Experiment 2 (0.56 MPa above methane hydrate dissociation pressure at 278 K), and 7.52 MPa in Experiment 3 (0.4 MPa above methane hydrate dissociation pressure at 283 K). For Experiment 1, gas phase methane concentration exceeded 77 mol% before methane hydrate dissociation pressure (2.72 MPa at 273.4 K) was reached. Complete methane hydrate decomposition was however achieved when system pressure dropped beyond methane hydrate dissociation pressure as evidenced by maximum gas phase methane concentration of 90.5 mol%. In Experiment 4, in the presence of nitrogen, maximum gas phase methane concentration of 71 mol% was achieved at 3.22 MPa (0.5 MPa above the methane hydrate dissociation pressure at 273.4 K). Comparison of experiments conducted at 273.4 K (Experiments 1 and 4)) shows that Experiment 4 (nitrogen injection) gave the highest methane recovery at any given pressure and also highest decomposition at pressures farthest from the methane hydrate decomposition pressure at 273.4 K. In general, final gas phase methane concentration is higher for experiments conducted at lower temperatures. However, in terms of percentage recovery, Experiment 3 (air injection at 283 K) gave the highest recovery, and decreases successively with decreasing temperature. Thus, it can be said that high temperatures favour the kinetics as well as the thermodynamics of methane recovery.

From the foregoing, it is evident that the injection of compressed air and nitrogen into methane hydrate-bearing sediments leads to methane hydrate decomposition at pressures above the methane hydrate dissociation pressures at the prevailing temperatures. A major benefit of this technique is significant improvement of the technical feasibility and economic viability of the conventional depressurisation method. Technically, injection of compressed air or nitrogen minimizes the extent of depressurisation required to decompose methane hydrate by directly shifting the HSZ, that is, the reservoir does not need to be depressurised

below the methane hydrate dissociation pressure. It also makes it possible to perform depressurisation in multiple stages, depending on the hydrate reservoir conditions. The minimised depressurisation leads to reduced drawdown between the production well and the reservoir, consequently, allowing better control of water and sand flow to the well. The high pressure gas production could also minimise the requirement for external pumps to lift produced water as obtainable in conventional depressurisation. Furthermore, this technique has the potential to improve the feasibility of methane recovery by depressurisation in gas hydrate reservoirs, especially in severe reservoir conditions such as low permeability or low hydrate saturations.

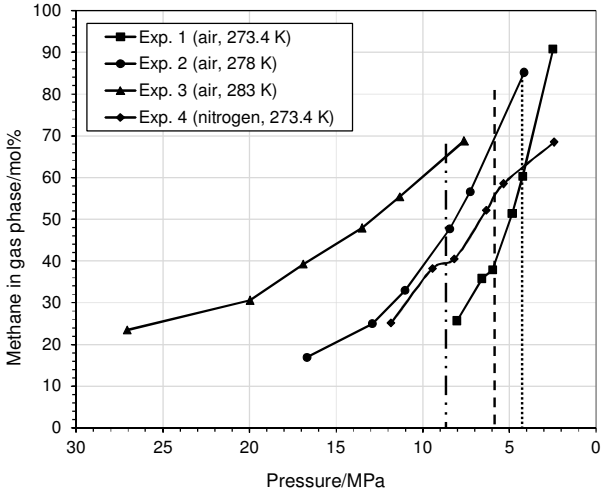

Figure 9 Gas phase methane concentration during the entire depressurisation phases in the presence of compressed air and nitrogen. The dotted, dashed, and dashed-dotted vertical lines represent the decomposition pressures of methane hydrate at 273.4 K, 278 K, and 283 K respectively. Methane hydrate starts to decompose well inside the methane hydrate stability zone.

5 Conclusions

Air and nitrogen injection into gas hydrate-bearing sediments was experimentally studied to enhance conventional depressurisation for methane recovery. Results of the experiments show that depressurisation can be conducted in multiple stages with different methane concentrations in gas phase. Air and nitrogen injection led to fast methane hydrate dissociation by shifting the methane hydrate stability zone. Kinetics study revealed a rapid rise in gas phase methane concentration within a short time interval in each stage. Air and nitrogen injection enhanced the depressurisation process, generating a methane-rich gas with more than 80 mol% methane at pressures above the methane hydrate dissociation pressure. Higher methane recoveries at high temperatures in the presence of the injected gas shows that high temperatures favour the kinetics as well as the thermodynamics of methane recovery. At similar conditions, nitrogen injection shows an improved methane recovery over air injection. This technique could substantially improve the technical feasibility and economic viability of conventional depressurisation method for methane recovery from gas hydrate reservoirs.

Acknowledgements

The authors would like to thank Skolkovo Institute of Science and Technology, Moscow, Russia for providing financial support for this work. The Petroleum Technology Development Fund (PTDF), Abuja, Nigeria is also acknowledged for the PhD scholarship of Anthony Okwananke.

References

[1] E.D. Sloan, C.A. Koh, Clathrate hydrates of natural gases, 3rd Edition, Taylor and Francis, 2007.
[2] K.A. Kvenvolden, Gas hydrates-geological perspective and global change, Rev. Geophys. 31 (1993) 173–187.
[3] A. V. Milkov, Global estimates of hydrate-bound gas in marine sediments: how much is really out there? Earth-Science Rev. 66 (2004) 183–197.
[4] A. V. Milkov, R. Sassen, Preliminary assessment of resources and economic potential of individual gas hydrate accumulations in the Gulf of Mexico continental slope, Mar. Pet. Geol. 20 (2003) 111–128. doi:10.1016/S0264-8172(03)00024-2.
[5] Z.R. Chong, G.A. Pujar, M. Yang, P. Linga, Methane hydrate formation in excess water

simulating marine locations and the impact of thermal stimulation on energy recovery, Appl. Energy. 177 (2016) 409–421.
[6] G.J. Moridis, T.S. Collett, S.R. Dallimore, T. Satoh, S. Hancock, B. Weatherill, Numerical studies of gas production from several CH_4 hydrate zones at the Mallik site, Mackenzie Delta, Canada, J. Pet. Sci. Eng. 43 (2004) 219–238.
[7] B. Li, X.-S. Li, G. Li, J.-C. Feng, Y. Wang, Depressurization induced gas production from hydrate deposits with low gas saturation in a pilot-scale hydrate simulator, Appl. Energy. 129 (2014) 274–286.
[8] L. Xiong, X. Li, Y. Wang, C. Xu, Experimental Study on Methane Hydrate Dissociation by Depressurization in Porous Sediments, Energies. 5 (2012) 518–530. doi:10.3390/en5020518.
[9] Y. Song, C. Cheng, J. Zhao, Z. Zhu, W. Liu, M. Yang, K. Xue, Evaluation of gas production from methane hydrates using depressurization, thermal stimulation and combined methods, Appl. Energy. 145 (2015) 265–277.
[10] Y.F. Makogon, F.A. Trebin, A.A. Trofimuk, V.P. Tsarev, N.V. Cherskiy, Detection of a pool of natural gas in a solid (hydrate gas) state, Dokl. Akad. Nauk SSSR. 196 (1972) 197–200.
[11] M. Kurihara, A. Sato, K. Funatsu, H. Ouchi, et al, SPE 132155 Analysis of Production Data for 2007 / 2008 Mallik Gas Hydrate Production Tests in Canada, in: CPS/SPE Int. Oil Gas Conf. Exhib., Beijing, China, 8-10 June, 2010.
[12] K. Yamamoto, Y. Terao, T. Fujii, T. Ikawa, M. Seki, M. Matsuzawa, T. Kanno, Operational overview of the first offshore production test of methane hydrates in the Eastern Nankai Trough, in: Offshore Technol. Conf., Houston, Texas, 2014: pp. 2007–2008.
[13] R. Boswell, T.S. Collett, The Gas Hydrates Resource Pyramid, Fire Ice US DOE NETL. 6 (2006).
[14] P. Linga, C. Haligva, S.C. Nam, J.A. Ripmeester, P. Englezos, Recovery of Methane from Hydrate Formed in a Variable Volume Bed of Silica Sand Particles, Energy & Fuels. 23 (2009) 5508–5516. doi:10.1021/ef900543v.
[15] L.G. Tang, R. Xiao, C. Huang, Z.P. Feng, S.S. Fan, Experimental Investigation of Production Behavior of Gas Hydrate under Thermal Stimulation in Unconsolidated Sediment, Energy and Fuels. (2005) 2402–2407.
[16] G.C. Fitzgerald, M.J. Castaldi, Thermal Stimulation Based Methane Production from Hydrate Bearing Quartz Sediment, Ind. Eng. Chem. Res. 52 (2013) 87–92.
[17] A.E. Nakoryakov, V. E., Misyura, S. L., Elistratov, S. L, Manakov, A. Yu. and Shubnikov, Combustion of Methane Hydrates, J. Eng. Thermophys. 22 (2013) 87–92.
[18] W.X. Pang, W.Y. Xu, C.Y. Sun, C.L. Zhang, G.J. Chen, Methane hydrate dissociation experiment in a middle-sized quiescent reactor using thermal method, Fuel. 88 (2009) 497–503.
[19] J. Zhao, C. Cheng, Y. Song, W. Liu, Y. Liu, K. Xue, Z. Zhu, Z. Yang, D. Wang, M. Yang, Heat Transfer Analysis of Methane Hydrate Sediment Dissociation in a Closed Reactor by a Thermal Method, Energies. 5 (2012) 1292–1308. doi:10.3390/en5051292.
[20] F. Dong, X. Zang, D. Li, S. Fan, D. Liang, Experimental Investigation on Propane Hydrate Dissociation by High Concentration Methanol and Ethylene Glycol Solution Injection, Energy & Fuels. 23 (2009) 1563–1567.
[21] T. Kawamura, Y. Sakamoto, M. Ohtake, Y. Yamamoto, H. Haneda, Dissociation Behavior of Hydrate Core Sample Using Thermodynamic Inhibitor, Int. J. Offshore Polar Eng. 16 (2006) 5–9.
[22] J. Lee, Experimental Study on the Dissociation Behavior and Productivity of Gas Hydrate by Brine Injection Scheme in Porous Rock, Energy & Fuels. 24 (2010) 456–463.

doi:10.1021/ef900791r.
[23] B. Tohidi, J. Yang, M. Salehabadi, R. Anderson, A. Chapoy, CO_2 Hydrates Could Provide Secondary Safety Factor in Subsurface Sequestration of CO_2, Environ. Sci. Technol. 44 (2010) 1509–1514.
[24] Y. Park, M. Cha, J. Cha, K. Shin, H. Lee, Swapping carbon dioxide for complex gas hydrate structures, in: 6th International Conference on Gas Hydrates (ICGH 2008) Vancouver, British Columbia, Canada 6-10 July, 2008.
[25] H. Kang, D. Koh, D. Kim, J. Park, M. Cha, H. Lee, Recovery of Methane Intercalated in Natural Gas Hydrate Sediments Using a Carbon Dioxide and Flue Gas Mixture, in: Twenty-second International Offshore and Polar Engineering Conference, Rhodes, Greece, 17-22 June, 2012.
[26] K. Shin, Y. Park, M. Cha, K. Park, D. Huh, J. Lee, S. Kim, H. Lee, Swapping Phenomena Occurring in Deep-Sea Gas Hydrates, Energy & Fuels. 22 (2008) 3160–3163. doi:10.1021/ef8002087.
[27] Y. Lee, Y. Seo, T. Ahn, J. Lee, J.Y. Lee, S.-J. Kim, Y. Seo, CH_4–Flue gas replacement occurring in sH hydrates and its significance for CH_4 recovery and CO_2 sequestration, Chem. Eng. J. 308 (2017) 50–58.
[28] D. Schoderbek, H. Farrell, K. Hester, J. Howard, K. Raterman, S. Silpngarmlert, K.L. Martin, B. Smith, P. Klein, ConocoPhillips Gas Hydrate Production Test Final Technical Report, 2013.
[29] D. Schoderbek, K.L. Martin, J. Howard, S. Silpngarmlert, K. Hester, North Slope Hydrate Field Trial: CO_2/CH_4 Exchange, in: Arct. Technol. Conf., Houston, Texas, USA, 3-5 Dec., 2012: pp. 1–17.
[30] H. Haneda, Y. Sakamoto, T. Kawamura, K. Aoki, T. Komai, Experimental study on dissociation behavior of methane hydrate by air, in: Proc. Fifth Int. Conf. Gas Hydrates, June 12-16, 2005. Trondheim, Norway.
[31] J.L. Panter, A.L. Ballard, A.K. Sum, E.D. Sloan, C.A. Koh, Hydrate Plug Dissociation via Nitrogen Purge: Experiments and Modeling, Energy & Fuels. 25 (2011) 2572–2578.
[32] H. Kang, D.-Y. Koh, H. Lee, Nondestructive natural gas hydrate recovery driven by air and carbon dioxide, Sci. Rep. 4 (2014) 6616. doi:10.1038/srep06616.
[33] Y. Ahn, H. Kang, D. Koh, H. Lee, Production of Natural Gas Hydrate by Using Air and Carbon Dioxide, Int. J. Chem. Mol. Nucl. Mater. Metall. Eng. 9 (2015) 796–800.
[34] X.-S. Li, B. Yang, G. Li, B. Li, Y. Zhang, Z.-Y. Chen, Experimental study on gas production from methane hydrate in porous media by huff and puff method in Pilot-Scale Hydrate Simulator, Fuel. 94 (2012) 486–494.
[35] X.-S. Li, B. Yang, L.-P. Duan, G. Li, N.-S. Huang, Y. Zhang, Experimental study on gas production from methane hydrate in porous media by SAGD method, Appl. Energy. 112 (2013) 1233–1240.
[36] G. Li, X.-S. Li, B. Yang, L.-P. Duan, N.-S. Huang, Y. Zhang, L.-G. Tang, The use of dual horizontal wells in gas production from hydrate accumulations, Appl. Energy. 112 (2013) 1303–1310.
[37] A. Okwananke, J. Yang, B. Tohidi, Experimental studies of methane recovery from methane hydrate in sediments by a combination of flue gas injection and depressurisation, in: Eight Int. Conf. Gas Hydrates, 28 July - 1 August, 2014. Beijing, China, 2014.
[38] J. Yang, A. Okwananke, B. Tohidi, E. Chuvilin, K. Maerle, V. Istomin, B. Bukhanov, A. Cheremisin, Flue gas injection into gas hydrate reservoirs for methane recovery and carbon dioxide sequestration, Energy Convers. Manag. 136 (2017) 431–438.
[39] R. Puri, D. Yee, Coalbed methane recovery using membrane separation of oxygen from air, 5388642, 1995.

[40] H. Haghighi, A. Chapoy, R. Burgess, B. Tohidi, Experimental and thermodynamic modelling of systems containing water and ethylene-glycol: application to flow assurance and gas processing. Fluid Phase Equilib. 276 (2009) 24-30.
[41] D.B. Robinson, D.-Y. Peng, The characterization of the heptanes and heavier fractions for the GPA Peng-Robinson programs, Gas Processors Association, Tulsa, Okla., 1978.

Highlights:

- Air/nitrogen injection approach was proposed to enhance depressurisation method.
- Multi-stage depressurisation was performed to recover methane from gas hydrates.
- Kinetics of methane release was investigated after injection of air and nitrogen.
- Methane-rich gas mixtures was produced inside methane hydrate stability zone.